Autoionization Mediated by Electron Transfer

Marko Förstel,[1,2] Melanie Mucke,[1] Tiberiu Arion,[1] Alex M. Bradshaw,[1,3] and Uwe Hergenhahn[1,*,†]

[1]*Max-Planck-Institut für Plasmaphysik (IPP), EURATOM Association, Boltzmannstr. 2, 85748 Garching, Germany*
[2]*Max-Planck-Institut für Kernphysik, Saupfercheckweg 1, 69117 Heidelberg, Germany*
[3]*Fritz-Haber-Institut der Max-Planck-Gesellschaft, Faradayweg 4- 6, 14195 Berlin, Germany*

(Received 7 October 2010; published 18 January 2011)

Electron-electron coincidence spectra of Ar-Kr clusters after photoionization have been measured. An electron with the kinetic energy range from 0 to approximately 1 eV is found in coincidence with the Ar 3*s* cluster photoelectron. The low kinetic energy electron can be attributed to an $Ar + Kr^+ + Kr^+$ final state which forms after electron transfer mediated decay. This autoionization mechanism results from a concerted transition involving three different atoms in a van der Waals cluster; it was predicted theoretically, but hitherto not observed.

DOI: 10.1103/PhysRevLett.106.033402 PACS numbers: 36.40.Mr, 34.70.+e, 79.60.Jv, 82.33.Fg

Recent investigations of excited ionized states in weakly bonded systems, e.g., in van der Waals clusters, have shown that the environment of an ion can actively take part in its deexcitation, giving rise to autoionization pathways which are not energetically possible for the isolated species. Interatomic Coulombic decay (ICD), for example, is a process in which an electron is emitted from a species in the immediate neighborhood of the initial vacancy, created, e.g., by photoionization [1–4]. Since its recent discovery, this process has received much attention, both for fundamental reasons and because of its interdisciplinary relevance [5]. Another autoionization process which can take place in heterogeneous systems is so-called electron transfer mediated decay (ETMD), first predicted theoretically by Cederbaum and coworkers [6]. In ICD, a concerted transition takes place, in which the vacancy created by photoionization is filled from the same atom or molecule and a neighboring entity within the cluster is ionized. In contrast, the initial vacancy in ETMD is filled via electron transfer from a neighboring atom or molecule. Autoionization can occur at either the electron donating species [ETMD(2)] or at a third, neighboring site [ETMD(3)] [7]. In the final state after ETMD(3), the initially ionized site has been neutralized and two vacancies have been created at two other, separated atoms or molecules. Both ICD and ETMD do not require the assistance of the nuclear dynamics in order to proceed, and are mediated solely by electron correlation [1,6–8]. It is clear that ETMD, which requires the transfer of an electron, can occur at observable levels only in systems where no other autoionization processes are energetically allowed [6].

Pernpointer *et al.* have considered in a theoretical study the autoionization of an $Ar^+(3s^{-1})$ vacancy after photoionization of an Ar-Kr_2 trimer [9]. They found that decay to an Ar^+-Kr^+-Kr state (ICD) is energetically not possible. The ionization energy of Kr is lower than that of Ar, however, so that doubly ionized states with both vacancies on Kr sites will have a lower binding energy. For a fixed electronic configuration of the two holes in the final state, another factor which influences the total final state energy is the Coulomb repulsion energy between them. This will decrease as the spatial separation between the two Kr atoms, on which the holes are located, increases. When considering the Ar-$(Kr^+)_2$ trimer, ETMD is not possible in a bent state, but in the linear Kr^+-Ar-Kr^+ configuration the final state energy is below the ionization energy of an Ar3*s* orbital. Thus, autoionization by ETMD becomes possible. The process is shown schematically in Fig. 1. A decay to states involving Kr^{2+} is not possible: Only due to the lowering of the Coulomb repulsion by the presence of two singly charged Kr atoms in the final state, can the double ionization threshold (DIP) decrease to a calculated value of DIP = 29 eV, which is below the single ionization energy of the $Ar^+(3s^{-1})$ state (30 eV). When more Kr atoms are added to the system, the ETMD efficiency increases, because more combinations of one Ar and two Kr atoms with a sufficiently large Kr-Kr separation are possible. The only competing relaxation mechanism for the $Ar^+(3s^{-1})$ vacancy is radiative decay by fluorescence, on a much longer time scale [10]. In this Letter we present the first direct experimental observation of the ETMD process. The particular process we demonstrate is ETMD(3) in medium-sized mixed Ar-Kr clusters, in which an Ar 3*s* vacancy autoionizes into a state containing two Kr^+ cations. In two earlier experiments the influence of ETMD on the results was discussed, but it could not be separated from competing mechanisms [11,12].

The experiment was performed on the beam line TGM4 of the BESSY II synchrotron radiation facility in Berlin, in single bunch mode operation. Ar-Kr clusters were produced by coexpansion of an ArKr mixture ($5 \pm 1\%$ Kr) through a conical nozzle (100μ diameter, 15° half opening angle) into an expansion chamber, which was separated from the main chamber by a conical skimmer [13]. The stagnation pressure was kept at 1.5 bar. The nozzle temperature was 118 K. It was shown earlier that a

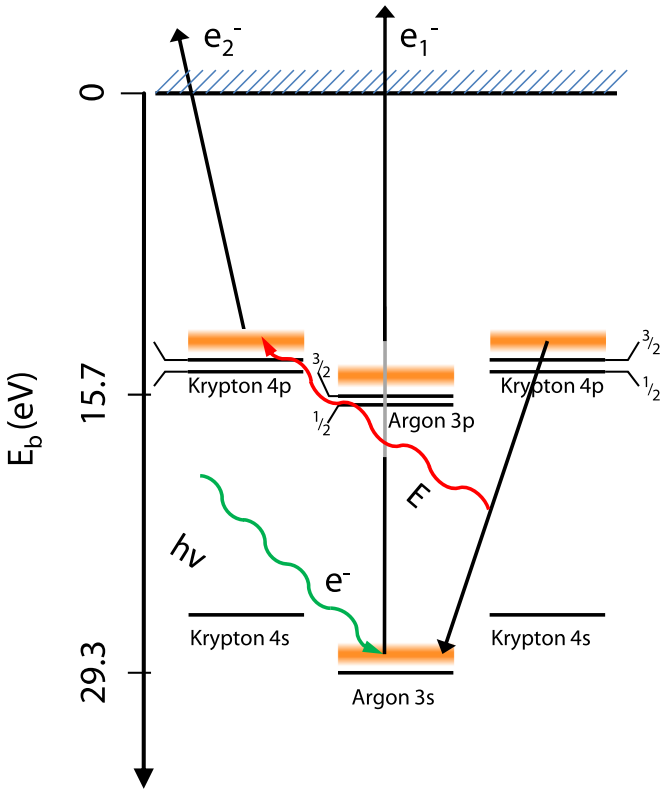

FIG. 1 (color online). Scheme of the ETMD(3) process. The solid, horizontal lines correspond to the monomer binding energies. The shaded bands designate the corresponding binding energies in a cluster. A vacancy in the Ar 3s cluster is created by photoionization, releasing electron e_1. The 3s band is filled via electron transfer from a neighboring Kr 4p cluster electron. At the same time, ionization occurs at a second, neighboring Kr atom which releases electron e_2. The final state fragments by Coulomb explosion (not shown).

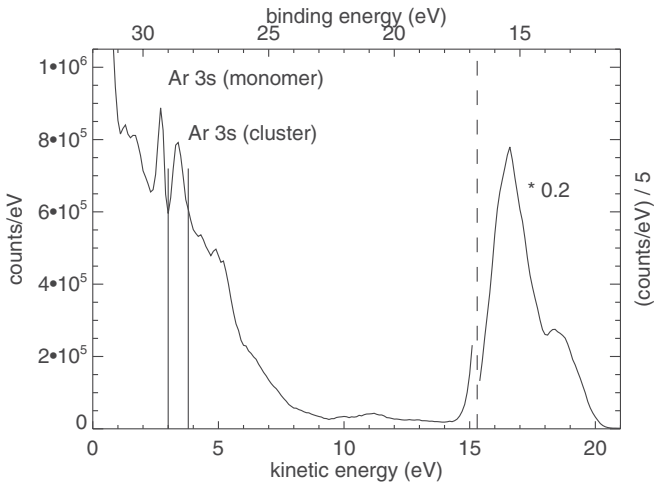

FIG. 2. Electron spectrum of mixed Ar-Kr clusters after photoionization at 32 eV photon energy. The two solid vertical lines indicate the region of the Ar 3s cluster photoelectron line; at the low kinetic energy side of it, the 3s photoline from uncondensed Ar atoms can be seen. Between 15 and 20 eV kinetic energy the Ar 3p and Kr 4p contributions can be seen. This part of the spectra has been scaled by a factor of 0.2. Intensity is given as counts per eV.

coexpansion of Ar and Kr leads to heterogeneous clusters which consist of a Kr core with Ar atoms on the surface [14]. All spectra were recorded using a magnetic bottle electron analyzer with an energy resolution of approximately $E/\Delta E = 20$. In order to efficiently detect electrons with kinetic energies down to less than 100 meV, a static acceleration potential of +2.2 V was used. Energy calibration was performed using a set of He 1s spectra.

The photoelectron spectrum of the mixed Ar-Kr cluster beam is shown in Fig. 2 for $h\nu = 32$ eV. The Ar 3p and Kr 4p photoelectron lines, which dominate the spectrum due to their large cross sections, are seen between 15 and 18 eV kinetic energy. The sharp feature at 2.7 eV kinetic energy is the Ar 3s monomer photoelectron line. At slightly higher kinetic energy, the Ar 3s cluster contribution is located [15] in the range of 3 to 3.8 eV. Compared to the calculations for the $ArKr_2$ trimer, the observed Ar 3s ionization energy is at a lower value. This can be attributed mainly, or even in total, to polarization effects, which partially shield the vacancy in the ionized state, thus leading to a reduced ionization energy [16]. The same energy lowering will also occur, however, for the ETMD final state. ETMD in larger Ar-Kr systems is therefore energetically also possible.

As in the case of ICD [3], the very low kinetic energy ETMD electron is difficult to detect on the background of secondary electrons, as shown in Fig. 2. It is therefore necessary to perform an experiment in which possible ETMD electrons are registered in coincidence with the Ar 3s cluster photoelectrons. Only in this way can incontrovertible evidence for the presence of this decay process be obtained. In Fig. 3 we present in the color-coded panel (b) the yield of electron pairs (e_1, e_2) recorded in such a coincidence experiment, also at $h\nu = 32$ eV. The color-coded panel shows the intensity of the recorded two-electron events vs kinetic energy of the first electron e_1 and the second electron e_2. In our experiment, the photoelectron always arrives first for the events we will identify with ETMD. The e_1 axis has therefore been converted to binding energy to aid in the interpretation of the photoelectron lines [see also top of Fig. 2]. The kinetic energy of the higher energy electron e_1 increases along the vertical axis, that of the lower energy electron e_2 along the horizontal. The right-hand panel (c) in Fig. 3 shows the intensity of all electron pairs summed along the energy axis of the second electron (e_2 axis) as a function of electron e_1 energy. Again, the 3s cluster photoelectron line is recognized as a sharp feature in the range between 3 and 3.8 eV kinetic energy (29 to 28.2 eV binding energy), sitting on an unstructured background in the kinetic energy range 0 to 6 eV (see below). When comparing this panel to Fig. 2 it should be noted that Fig. 3 derives only from those events in which two electrons were recorded, while Fig. 2 also contains

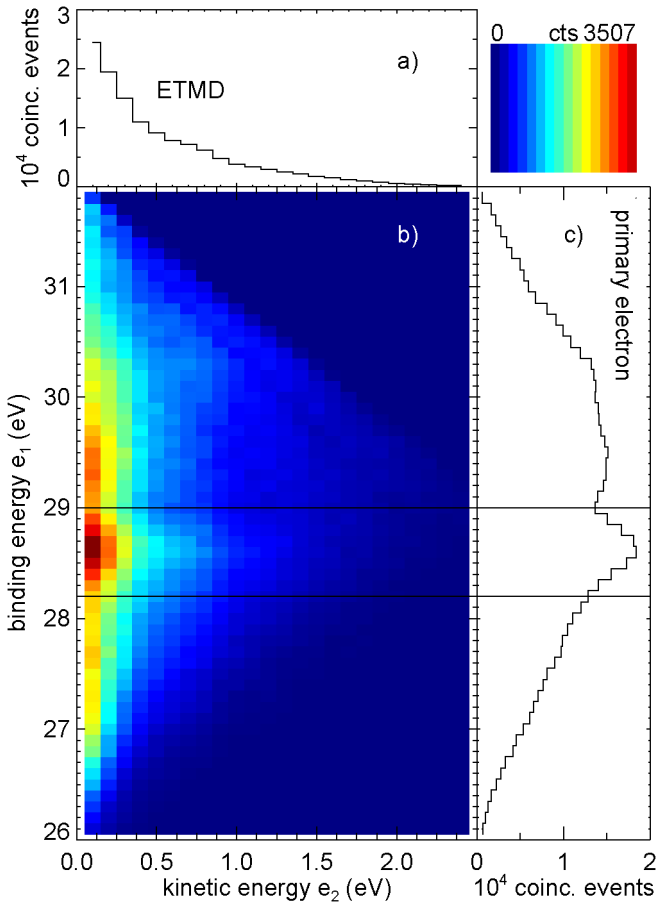

FIG. 3 (color online). Electron-electron coincidence spectrum after photoionization of mixed Ar-Kr clusters at $h\nu = 32$ eV. The black horizontal lines in the color-coded map, panel (b), and in panel (c) mark the energy region of the Ar 3s cluster electron [compare to Fig. 2]. The right-hand panel (c) shows the projection of all counts onto the axis of e_1, which corresponds to the kinetic energy spectrum of all primary electrons that contribute to the emission of secondaries. The upper panel (a) shows the projection of all events within the marked region onto the axis of e_2. This corresponds to the kinetic energy spectrum of all slow electrons appearing in coincidence with an Ar 3s cluster photoelectron, that is, all electrons which result from ETMD. Primary processes other than Ar 3s photoionization may contribute some of the intensity in panel (a). See text for details. Intensity is given as events per pixel, with a width of 100×100 meV.

those events corresponding to the detection of a single electron. This is the reason why the atomic 3s line is not visible in panel (c) of Fig. 3, as 3s photoemission in atomic species does not lead to emission of a second electron. Compared to Fig. 2, the background of inelastically scattered electrons at very low energies in Fig. 3 is also reduced.

The e_1 range between 3 and 3.8 eV kinetic energy, which corresponds to the region where the Ar 3s cluster photoelectron is expected, is marked by two horizontal lines. It can be seen in the central panel (b) of Fig. 3 that in coincidence with the Ar 3s cluster photoelectron a second electron is detected, with a kinetic energy range from 0 to approximately 1 eV kinetic energy, with the maximum of its contribution below 0.2 eV kinetic energy [see panel (a) in Fig. 3].

We identify the low energy electron detected following Ar 3s cluster photoionization with the continuum electron emitted via the ETMD(3) process, since this is the only autoionization process that is energetically allowed for an Ar 3s vacancy in this system. Other allowed double ionization processes proceed via simultaneous photo-double-ionization or by inelastic scattering, and lead to different signatures in the electron-electron coincidence map (see below). In a control experiment on a pure Ar cluster jet (not shown), no secondary electrons are observed in coincidence with a 3s primary photoelectron, in support of this interpretation of our data.

The energy balance for the ETMD electron includes its kinetic energy, the corresponding initial and final state energies and the energy imparted to kinetic energy of the nuclear fragments after the autoionization process. The latter can be calculated from $E_{\mathrm{kinETMD}} = h\nu - E_{\mathrm{DIP}} - E_C$, where E_{DIP} denotes the double ionization potential and E_C is the kinetic energy release to the nuclear fragments after a Coulomb explosion of the doubly ionized cluster. We observe a kinetic energy range of approximately $E_{\mathrm{kinETMD}} = 0 \ldots 1$ eV. Knowing that $E_{\mathrm{DIP}} = 29$ eV, [9], we calculate a kinetic energy of the cluster fragments of approximately $E_C = 2 \ldots 3$ eV. This is within the expected range.

We now address the unstructured feature underlying the Ar 3s + ETMD coincidence events. This can be explained by two other double ionization mechanisms occurring in a similar energy range. The first one is the ICD of $KrKr^{+*}$ satellite states, as observed by Lablanquie *et al.* for pure Kr dimers [17]. The lowest photon energy for which ICD was observed in the dimer experiments is 31.15(10) eV, in good agreement with calculations [9]. Considering that the Kr core of our clusters consists of more than two atoms, this threshold might be lower. Using a Kr-Kr distance of 4 Å [9] and outer valence binding energies observed for larger clusters [15], an estimate for the Kr ICD final state energy is 29.6 eV. As the region above 29 eV binding energy is covered by a dense band of satellite states [17], we suggest that ICD of these states is energetically possible in larger clusters, and indeed contributes to the structure seen in Fig. 3 at e_1 values between 0 and 3 eV, i.e., at binding energies between 32 and 29 eV. A second contribution to the unstructured part of the coincidence spectrum may result from intracluster electron-electron scattering involving two Kr 4p electrons, or one Kr 4p and one Ar 3p electron. This leads to a total kinetic energy of the two resulting electrons of approximately 5 to 6 eV, not taking into consideration energy sharing with ionic fragments due to the Coulombic fission of the cluster. The kinetic energy can be arbitrarily distributed among the two resulting electrons. This process is visible in a high contrast coincidence

map as a diagonal feature along the lines of constant total energy. The intensity of the two effects mentioned is, however, not high enough to explain the whole background, which implies that further, as yet unidentified effects might play a role in the observed spectrum.

We would like to stress the relevance of our results in a broader context. The established picture for electron transfer reactions explains their occurrence by way of spontaneous fluctuations in the nuclear coordinates, such that values of these coordinates are reached which satisfy the Franck-Condon and energy conservation conditions [18]. Alternatively, an electron tunneling (hopping) model has been proposed which can be extended to describe the stepwise migration of electrons or holes along, for example, a peptide chain (e.g., [19]). In strong contrast to both of these mechanisms, ETMD is a charge transfer process driven solely by electron correlation and relaxation. The charge transfer effectuated by electron correlation has been discussed in pioneering experimental [20] and theoretical [21,22] papers. It occurs on a very fast time scale and its analysis can be carried out at fixed positions of the nuclear coordinates. Breidbach and Cederbaum refer to this mechanism as ''charge migration.'' Arguably, ETMD is so far the most transparent demonstration of the effect, which—taken in perspective—may lead to a change of paradigm.

Summarizing, we have given clear experimental evidence for the occurrence of ETMD(3) in mixed Ar-Kr clusters. In this autoionization process, which so far was only investigated by theory, three different sites in a weakly bonded cluster contribute and are connected by electron correlation. We have measured the kinetic energy spectrum of the ETMD electron using electron-electron coincidence spectroscopy. Its maximum intensity occurs at energies below 0.2 eV and its maximum energy is reached at about 1 eV. No other nonradiative decay channels of the $Ar^+(3s^{-1})$ state are allowed in the system considered here, thus allowing ETMD to be observed.

We acknowledge fruitful discussions with Antje Vollmer, the research group of Lenz Cederbaum, and, in particular, with Nicolas Sisourat. The contribution of Hans-Peter Rust to data acquisition is also acknowledged. This work has been supported by the Deutsche Forschungsgemeinschaft, the Advanced Study Group of the Max-Planck-Society, and the Fonds der chemischen Industrie.

Note added.—An independent observation of ETMD in triply ionized Ar dimers has been very recently described [23].

*c/o Helmholtz-Zentrum Berlin, Albert-Einstein-Str. 15, 12489 Berlin, Germany.

†uwe.hergenhahn@ipp.mpg.de

[1] L. S. Cederbaum, J. Zobeley, and F. Tarantelli, Phys. Rev. Lett. **79**, 4778 (1997).

[2] S. Marburger, O. Kugeler, U. Hergenhahn, and T. Möller, Phys. Rev. Lett. **90**, 203401 (2003).

[3] M. Mucke, M. Braune, S. Barth, M. Förstel, T. Lischke, V. Ulrich, T. Arion, U. Becker, A. Bradshaw, and U. Hergenhahn, Nature Phys. **6**, 143 (2010).

[4] T. Jahnke, H. Sann, T. Havermeier, K. Kreidi, C. Stuck, M. Meckel, M. Schöffler, N. Neumann, R. Wallauer, S. Voss, A. Czasch, O. Jagutzki, A. Malakzadeh, F. Afaneh, T. Weber, H. Schmidt-Böcking, and R. Dörner, Nature Phys. **6**, 139 (2010).

[5] U. Hergenhahn J. Electron Spectrosc. Relat. Phenom. (to be published).

[6] J. Zobeley, R. Santra, and L. S. Cederbaum, J. Chem. Phys. **115**, 5076 (2001).

[7] C. Buth, R. Santra, and L. S. Cederbaum, J. Chem. Phys. **119**, 10575 (2003).

[8] I. B. Müller and L. S. Cederbaum, J. Chem. Phys. **122**, 094305 (2005).

[9] M. Pernpointer, N. V. Kryzhevoi, and S. Urbaczek, J. Chem. Phys. **129**, 024304 (2008).

[10] A. Hibbert and J. E. Hansen, J. Phys. B **27**, 3325 (1994).

[11] K. Kreidi, T. Jahnke, T. Weber, T. Havermeier, X. Liu, Y. Morisita, S. Schössler, L. P. H. Schmidt, M. Schöffler, M. Odenweller, N. Neumann, L. Foucar, J. Titze, B. Ulrich, F. Sturm, C. Stuck, R. Wallauer, S. Voss, I. Lauter, H. K. Kim, M. Rudloff, H. Fukuzawa, G. Prümper, N. Saito, K. Ueda, A. Czasch, O. Jagutzki, H. Schmidt-Böcking, S. Stoychev, P. V. Demekhin, and R. Dörner, Phys. Rev. A **78**, 043422 (2008).

[12] M. Hoener, D. Rolles, A. Aguilar, R. C. Bilodeau, D. Esteves, P. Olalde Velasco, Z. D. Pesic, E. Red, and N. Berrah, Phys. Rev. A **81**, 021201 (2010).

[13] M. Mucke, M. Förstel, and U. Hergenhahn *et al.* (to be published).

[14] M. Lundwall, H. Bergersen, A. Lindblad, G. Öhrwall, M. Tchaplyguine, S. Svensson, and O. Björneholm, Phys. Rev. A **74**, 043206 (2006).

[15] R. Feifel, M. Tchaplyguine, G. Öhrwall, M. Salonen, M. Lundwall, R. R. T. Marinho, M. Gisselbrecht, S. L. Sorensen, A. Naves de Brito, L. Karlsson, N. Mårtensson, S. Svensson, and O. Björneholm, Eur. Phys. J. D **30**, 343 (2004).

[16] O. Björneholm, F. Federmann, F. Fössing, T. Möller, and P. Stampfli, J. Chem. Phys. **104**, 1846 (1996).

[17] P. Lablanquie, T. Aoto, Y. Hikosaka, Y. Morioka, F. Penent, and K. Ito, J. Chem. Phys. **127**, 154323 (2007).

[18] R. S. Marcus, Nobel lecture.

[19] C. Shih, A. K. Museth, M. Abrahamsson, A. M. Blanco-Rodriguez, A. J. Di Bilio, J. Sudhamsu, B. R. Crane, K. L. Ronayne, M. Towrie, A. Vlcek, Jr., J. H. Richards, J. R. Winkler, and H. B. Gray, Science **320**, 1760 (2008).

[20] R. Weinkauf, P. Schanen, A. Metsala, E. W. Schlag, M. Burgle, and H. Kessler, J. Phys. Chem. **100**, 18567 (1996).

[21] J. Breidbach and L. S. Cederbaum, J. Chem. Phys. **126**, 034101 (2007) and references therein.

[22] G. Periyasamy, R. D. Levine, and F. Remacle, Chem. Phys. **366**, 129 (2009).

[23] K. Sakai *et al.*, Phys. Rev. Lett. 106 033401 (2011).